



Acquisition of Current and Vibration Data for Rewound Burnt Three-Phase Induction Motor

***ABDULLATEEF, AI; FAGBOLAGUN, OS; SANUSI, MF**

Department of Electrical and Electronics Engineering, University of Ilorin, Ilorin, Kwara State, Nigeria
**Corresponding Author Email: abd_lateef.aai@unilorin.edu.ng*

ABSTRACT: Induction motors are used in the industries for various applications because they are reliable and rugged. However, late detection of faults and inappropriate maintenance of the machine often leads to damage of the windings which results in production losses and outright replacement. This study presents the use of a data acquisition system (DAS) to acquire current and vibration data of re-designed and re-wound burnt three-phase induction motor for the purpose of the motor faults analysis. The designed number of turns per pole per phase is 253 turns which were distributed in four slots per phase at 64, 63, 63 and 63 turns respectively. The DAS developed was used to acquire the current and vibration data at both normal and fault conditions through tapings prepared for the purpose. The average value of normal current data in the red, yellow and blue phases from the sampled data are 3.4 A, 3.1 A and 2.7A respectively. The average currents during short circuit between phase A and phase B are 11.3 A and 12.2 A respectively while vibration fault data stands at 1.62. Also, for the inter-turn short circuit in phase A, the average value of the currents in the phases are 12.1A, 3.1A and 2.7A respectively. The Mean Square Error value of the acquired and measured data is 0.00002.

DOI: <https://dx.doi.org/10.4314/jasem.v23i12.15>

Copyright: Copyright © 2019 Abdullateef *et al.* This is an open access article distributed under the Creative Commons Attribution License (CCL), which permits unrestricted use, distribution, and reproduction in any medium, provided the original work is properly cited.

Dates: Received: 30 November 2019; Revised: 20 December 2019; Accepted: 23 December 2019

Keywords: three-phase induction motor, data acquisition system, stator winding design, microcontroller.

Induction motors are broadly used in industries among electric machines because they are reliable and rugged. Thus, they are referred to as the workhorse of industries due to their use in various applications. Natural ageing and other factors such as misuse, late detection of faults and inappropriate maintenance of this machine often lead to repair or damage which results in production losses and outright replacements (Al-Ali and Dabbousi, 2013). These losses may be prevented or reduced if the conditions of the motor are monitored in real time rather than conventional manual inspection/testing. The cost incurred due to unexpected breakdown could be very high as a lot of other equipment depend on continuous and parallel operation of induction motors in the industries (Subha, 2018). Hence, there is a need for adequate real time monitoring and fault diagnoses in order to prevent damage and total breakdown since induction motors are expensive to replace. Real time monitoring is possible if data of parameters relating to the performance of the machines are acquired and processed. Among several parameters that can aid fault analysis/monitoring of the machine, current and vibration data stand out and play a significant role in that they give an opportunity to diagnose, in advance, any faults or failures in the machines (Doolan *et al.*, 2017). Thus, the availability of these parameter's data

are important to studying the machine's characteristic and behaviour which, are necessary indices for fault monitoring and detection. One of the most common faults in induction motors is the stator fault which accounts for 30-40% of failures in the machine (Siddique *et al.*, 2005). Stator fault could be as a result of a failure in the stator winding which includes phase to phase short circuit and inter-turn short circuit. These faults need to be detected at the incipient stage before they damage the machine windings and consequently break down the motor. To achieve this, the current and vibration data that give vital information about the status of the machine, for both normal and faulty operating conditions are required. These data can be accessed using the data acquisition system. Data acquisition system (DAS) involves the sampling of signals which measure real world physical conditions and converting the sampled signal into numeric values that can be understood and operated upon by computer systems. It is made up of sensors/transducers, communication links, signal processing units, computers, database and software (Ofei, 2010; Park *et al.*, 2003). Various studies have proposed different DAS for different purposes. (Fisher and Gould, 2012; Lockridge *et al.*, 2016; Mandal and Singh, 2017; Sarma *et al.*, 2018). Although, there exist data acquisition equipment and

*Corresponding Author Email: abd_lateef.aai@unilorin.edu.ng

data logger which could be used to acquire current and vibration data from the machine as well as log the data into a storage device or computer system, these are often expensive and out of reach when required for laboratory experiments. This has necessitated the need to develop a low-cost data acquisition system that can work efficiently for acquiring these data as well as processing them for further usage. In this study, a DAS based on microprocessor is developed to acquire the current and vibration data of the induction motor. Accordingly, the objective of this study is to design and develop a data Acquisition system for current and vibration data of rewound burnt three-phase induction motor for fault analysis.

MATERIALS AND METHODS

Three-phase Induction Motor Winding Development: Stator winding is significant in the operation of an induction motor in that they produce the magnetic field required for electromagnetic induction to take place in the induction motors when excited by voltage source (Gupta, 2009). In this study, the winding of a bad/burnt/disuse three-phase motor was re-designed and rewound in order to simulate faults and acquire the data of such faults for the analysis and performance of the motor.

Table 1: Measured values from disused motor

Symbol	Meaning	Dimension (mm)
L_s	Axial stator Length	85
D_s	External diameter of stator	125
D	Bore diameter of stator	75.5
w_1, w_2	Width of stator slot	$w_1 = 6.621, w_2 = 8.5$
h_s	Height of stator slot	13.3
w_0	Opening of stator slot	2
h_n	Height of slot "neck"	0.64
w_t	Tooth width	3.98

Table 2: Winding factor of different phase slot

S_p	1	2	3	4	5	6	7	8
K_{wl}	1	0.966	0.960	0.958	0.957	0.956	0.956	0.955

Source: ("Neven Srb Elektromotor" by Pogoni, 2007) and (instructable by Niko)

(e) Magnetic flux per pole, Φ

$$\Phi = \frac{B_\phi \times d_p \times 10^{-4}}{1.57} \quad (4)$$

(f) Winding Factor

Three phase induction motor (TPIM) consists of three stator windings designed to operate at the same voltage levels. The design is affected by various constraints such as thermal limit and utility of stator slots. To design the number of winding in a machine, the bore diameter and axial length of the machine's stator are essential. These values were measured from the bad motor via the vernier calliper and tabulated in Table 1.

Relevant mathematical equations for the winding design

(a) Number of pole pairs, P

$$P = \frac{60 \times f}{N_s} \quad (1)$$

Where P is the number of pole pairs, f is the nominal frequency and N_s is the rotation speed of the magnetic filed

(b) Number of slots per pole and phase, S_p

$$S_p = \frac{S}{2 \times P \times m} \quad (2)$$

Where S_p is the number of slot per pole and phase; S is the number of slot; P is the number of pole pairs and m is the number of phases in winding

(c) Cross section area of teeth of one pole (cm^2), A_t

$$A_t = \frac{S \times w_t \times l_z}{2 \times P} \quad (3)$$

l_z = clean iron length

(d) Yoke cross sections area (cm^2), A_y
 Yokecrosssection=heightof stator yoke
 × clean iron length

Clean iron length is conventionally assumed to be 80.04 for stators.

Table 2 shows the winding factor and their corresponding number of slots per pole.

Winding factor $K_{wl} = 0.958$ corresponding to number of slot per pole and phase, $S_p = 4$

(g) Number of turns N_t

Number of turns is a function of the working voltage, the flux and some constants, is derived from the output equation expressed as

$$\text{Output in KVA} = 3 \times (V_p) \times (I_p) \times 10^{-3} \quad (5)$$

Where the input voltage per phase V_p is expressed as

$$V_p = 4.44 f N_t \Phi K_{wl}$$

$$\text{KVA} = 3 \times 4.44 f N_t \Phi K_{wl} \times I_p \times 10^{-3} \quad (6)$$

$$N_t = \frac{V_p}{4.44 \times f \times \Phi \times K_{wl}} \quad (7)$$

Φ is flux/pole,
 f is the nominal frequency (Hz)

(h) Number of turns per phase;
 = number of turns/phase/pole \times number of pole

(i) Number of turns per slot;
 = $\frac{\text{No of conductor per phase per pole}}{S_p} \quad (8)$

(j) Total number of turns in the whole slots;
 = Number of turns per phase \times number of ph

(k) Conductor Size
 Having calculated the number of turns per pole, next is the selection of the conduction size. This could be achieved using the slot fullness approach. Slot fullness approach uses the slot surface as well as the filling factor

(l) Slot surface, A_u
 Slot surface depends on the shape of the slot

$$A_u = \frac{\pi}{8} (w_1^2 + w_2^2) + \frac{h}{2} (w_1 + w_2) \quad (9)$$

(m) Determine the Filling Factor

Figure 2. Show the graph for selecting suitable filling factor (Instructable by Niko)

Filling factor of 0.34 was selected from the graph above based on the slot surface A_u of 93.4. Filling factor must be between the upper and bottom recommended line.

(n) Cross section area of the wire, A_v

$$A_v' = \frac{A_u \times f_u}{S_u'} \quad (10)$$

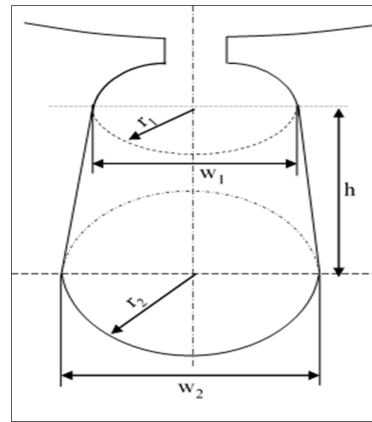


Fig 1: Stator Slot Surface

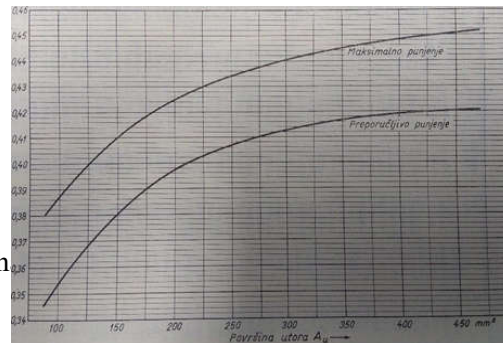


Fig 2: Graph of filling factor

Where A_v is the cross section of the wire, A_u is the slot surface, f_u is the filling factor and S_u is the number of turns in gap

(o) Thickness of wire, D

$$D = 2 \times \sqrt{\frac{A_v'}{\pi}} \quad (11)$$

Using equations 1 to 11, the values of the re-designed motor is shown in Table 3 while the winding development is illustrated in Figure 3.

Table 3: Design characteristics of re-designed induction motor.

S/N	Parameters	Values
1	Number of pole pair	1
2	Number of slots per pole per phase	4
3	Winding Factor	0.9804
4	Number of turns per pole per phase	253
5	Number of turns per slot	63
6	Slot surface	93.4mm
7	Winding Filling Factor	0.34
8	Cross section area of the wire	0.504mm ²
9	Diameter of the wire	0.8mm

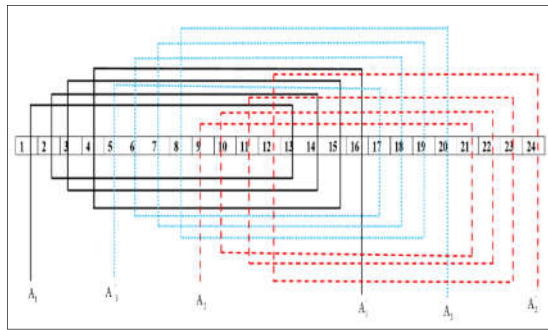


Fig 3: Stator Winding Layout development

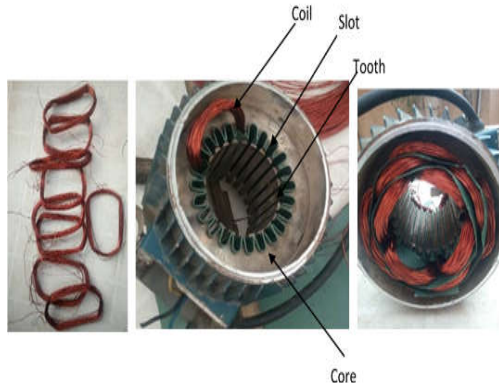


Fig 4: Inserting Formed Wound Coils in Stator

The rewound motor involves disassembly of the motor; removal of windings; insulation of the slots; coil making; insertion of the coil into the appropriate

slots; making necessary tapping for fault simulation and connection. Some of these steps are illustrated in Figure 4. Materials and tools used to achieve the aforementioned steps are copper wire, lacquer insulation (slot liner), thread, plier, coil packer, wood hammer, scissors, spanner, soldering iron and winding machine.

The motor was coupled after various connections and necessary fault simulations tapping have been extended out from the motor. In the process, adequate care was taken not to damage the most delicate parts such as winding insulation. In addition, ground and open circuit tests were carried out to ascertain the functionality of the motor before it was connected to the power source.

Data Acquisition System for Current and Vibration Data: Data acquisition system was developed for the rewound induction motor. It consists of four steps; circuit design and components layout; selection of appropriate components; programming and compilation of the programmed code on the Arduino board; Calibration of sensors and testing of the DAQ system. Figure 5 shows the block diagram of the experimental set up for data acquisition. The data of interest that were acquired are the current and vibration data that signifies the status of the machine in real time.

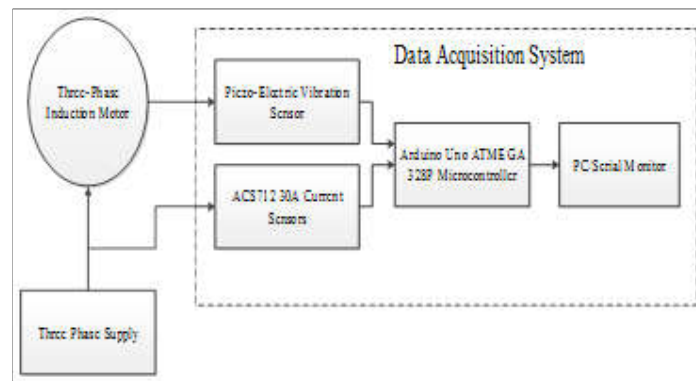


Fig 5. Data Acquisition Block Diagram

An Arduino Uno board based on Atmega328p chip microcontroller was used as the main signal processor. It consists of fourteen digital input/output pins, six of which can be used as pulse width modulation outputs. It also has six analogue inputs, each having a resolution of 10 bits and 16 MHz crystal oscillator which supplies the desired frequency to the system. It operates on a power supply of 5V and has a 32kB flash

memory (Atmega328p, 2015). An analogue current sensor ACS712ELC-30A (range: $\pm 30A$ based on the output of 66mV/A) shown in Figure 6 was used. (ACS712 Datasheet, 2007). The MEAS Vibration sensor used is a piezoelectric film which generates a certain level of voltage with mechanical strain. It generates approximately 0.2V per micrometre of movement it is subjected to (MEAS-SPEC, 2010).

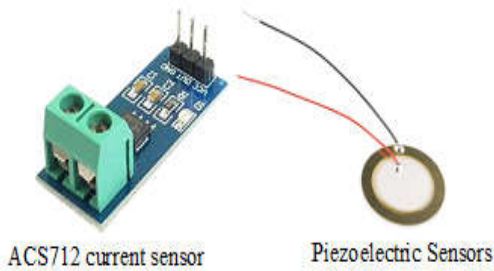


Fig 6: ACS712 and Piezoelectric Sensors

Figure 7 shows the circuit diagram of the DAQ device. Three current sensors, ACS712 of 30A range are connected to the analogue pins of the Arduino board, A1, A2 and A3 in series to the machine. The piezoelectric film is also connected to an analogue

input through $1M\Omega$ resistor which serves as a current limiter for the Arduino board in order to prevent the board from exceeding the 5V handling limit. The voltage data read by the Arduino board is in bits and was converted into voltage using equation 12

$$V_{out} = \frac{reading \times 5}{1023} \quad (12)$$

Where V_{out} represents the output voltage produced by the piezo-disk.

The Arduino board operates based on 9V voltage supply and manage the data readings of the sensors with Atmega328p chip as a controller and signal processor.

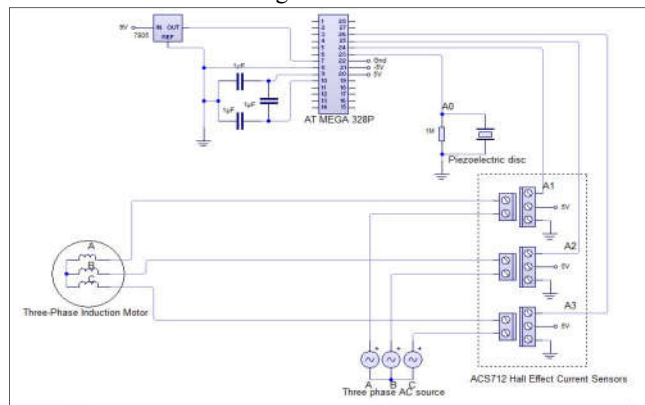


Fig 7: Complete Circuit Diagram

Figure 8 shows a display of the programming code written in C++ language in the Arduino IDE software (Arduino Products, 2019).

```

VIB_AND_CRT_SENSR | Arduino 1.8.9
File Edit Sketch Tools Help
VIB_AND_CRT_SENSR g
int LED_Pin = 24;
//int Vibr_Pin =A0;
const int VibSensor = A0;
int crt1 = A1;
int crt2 = A2;
int crt3 = A3;
const int threshold = 100; // threshold value
float vout = 0.0;
int sensorReading = 0; // variable to store the value read from the sensor pin
//current sensor calibration
int mVperAmp1 = 66; // use 100 for 20A Module and 66 for 30A Module
double Voltage1 = 0;
double VRMS1 = 0;
double AmperRMS1 = 0;
//current sensor calibration
int mVperAmp2 = 66; // use 100 for 20A Module and 66 for 30A Module
double Voltage2 = 0;
double VRMS2 = 0;
double AmperRMS2 = 0;
//current sensor calibration
int mVperAmp3 = 66; // use 100 for 20A Module and 66 for 30A Module
double Voltage3 = 0;
double VRMS3 = 0;
double AmperRMS3 = 0;
//current sensor calibration
float getVFF1[10];
    
```

Fig 8: Screenshot of Arduino IDE

The programming code was uploaded unto the Arduino board via a USB cable after it was debugged for any error. The acquired data is transferred from the board through the USB cable as well.

Test rig: Figure 9 shows a picture of the DAQ experimental setup. It consists of a 1.5hp three-phase rewind induction motor with its

windings extended on each phase for the purpose of short circuit faults simulation. the current sensors are connected in series with the induction machine and the vibration sensor is attached directly to the surface of the machine. The Arduino board was connected to the PC through a USB cable for programming code uploading and data acquisition. The acquired data is displayed on the computer in the Arduino IDE environment through its serial monitor.

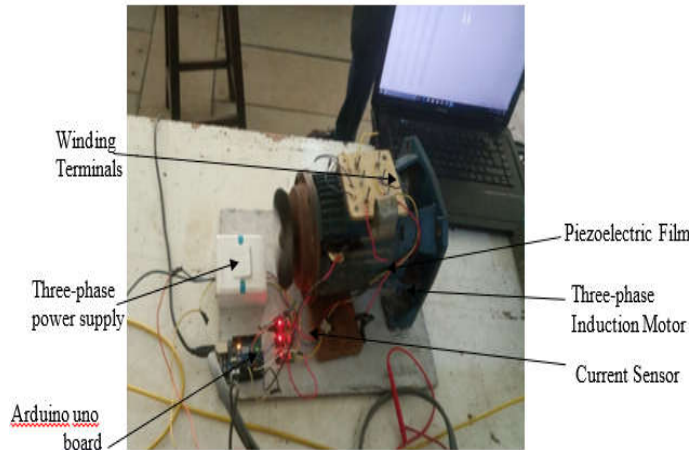


Fig 9: Experimental Test Rig

RESULTS AND DISCUSSIONS

The samples of current and vibration data acquired via the developed data acquisition system are shown in Table 4 to Table 6.

Table 4. Sample of Acquired data under normal condition

Normal condition				
Red phase current (A)	Blue phase current (A)	Yellow phase current (A)	Vibration	Time (ms)
3.37	3.09	2.72	1.1	3032
3.37	3.11	2.72	1.03	6132
3.4	3.11	2.72	1.1	9234
3.4	3.16	2.67	0.91	12335
3.4	3.11	2.72	0.91	15436
3.37	3.09	2.72	0.91	18538
3.35	3.09	2.72	0.89	21638
3.35	3.06	2.72	0.89	24738
3.37	3.06	2.72	1.01	27840
3.37	3.06	2.67	0.71	30941
3.4	3.09	2.67	1.12	34041

Table 5. Sample of acquired data under an inter-turn fault condition in the red phase

Inter-turn fault condition in phase A				
Red phase current (A)	Blue phase current (A)	Yellow phase current (A)	Vibration	Time (ms)
11.15	3.09	2.72	1.58	151886
12.12	3.11	2.72	1.86	154988
13.26	3.11	2.72	1.76	158089
12.81	3.16	2.67	1.91	161191
11.56	3.11	2.72	1.87	164293
12.27	3.09	2.72	1.73	167394
12.56	3.09	2.72	1.91	170494
11.54	3.06	2.72	1.87	173596
12.35	3.06	2.72	2.02	176698
12.45	3.06	2.67	1.91	179799
12.11	3.09	2.67	1.88	182900
11.56	3.09	2.72	1.88	186002

In particular, Table 4 shows the normal current and vibration data. It is observed that the current values in the phases are not the same. The red phase ranges from 3.35 to 3.4 ampere while the blue phase is from 3.06 to 3.11 ampere.

The yellow phase reading is the lowest and ranges between 2.67 and 2.72 amperes. This is not unconnected to the unbalance in the value of the three phases supply voltages. In addition, the vibration data is between 0.71 and 1.12. Table 5 shows the current and vibration data during the inter-turn fault in the red phase. It is observed that the current values in the shorted phase increases abnormally and ranges from 11.15 to 12.81 amperes while the blue and yellow phase reading remains normal. In addition, the vibration data under this fault increases and ranges from 1.58 to 2.02. Table 6 shows the current and vibration data during phase to phase fault in red and blue phase. During phase to phase fault, the current in the red phase ranges from 9.99 to 13.09 ampere and the blue phase ranges from 11.10 to 12.65 amperes, while the yellow phase current remains normal. In addition, the vibration data under this fault increases and ranges from 1.56 to 1.78.

Data Validation: The values of the current data were validated with a standard digital multimeter to get rid of possible discrepancies in the reliability of acquired data. The sample of the data is plotted in Figure 10 and the validation error based on Mean Square Error is 2×10^{-5} .

Conclusion: A three-phase induction motor stator winding has been re-designed and rewound for the purpose of stator phase-to-phase and inter-turn short circuit faults analysis. Data acquisition system was developed and used to acquire the current and vibration data under both normal and faults conditions.

The acquired data were validated and would be useful for the study of stator faults analysis of the three-phase induction motor.

Table 6. Sample of acquired data under phase to phase short circuit condition in red and blue phases.

Phase-to-phase short circuit condition				
Red phase current (A)	Blue phase current (A)	Yellow phase current (A)	Vibration	time (ms)
13.09	12.35	2.72	1.56	158089
11.04	12.58	2.72	1.67	161191
10.33	11.74	2.72	1.73	164293
12.32	11.1	2.67	1.43	167394
10.93	12.03	2.72	1.68	170494
9.99	12.42	2.72	1.63	173596
10.09	12.45	2.72	1.4	176698
11.38	12.32	2.72	1.78	179799
11.6	12.65	2.72	1.75	182900
12.63	12.49	2.67	1.62	186002
11.25	12.05	2.67	1.62	189103

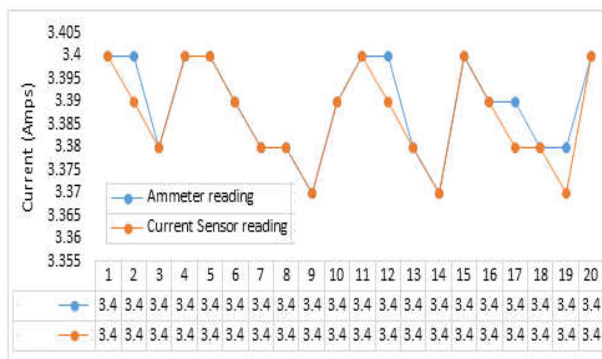


Fig 10: Current sensor validation

REFERENCES

Al-Ali, S; Dabbousi, R (2013). Rotor hot spot detection and resolution in large oil and gas industry motors. *Industry Applications Society 60th APCIC*, 1–8. IEEE.

Doolan FJ; Carvalho, SF; Cipriano MG; Salazar, A; de Paiva, J (2017). Wireless monitoring of induction machine rotor physical variables. *Sensors*, 17(11), 2660.

Fisher, DK; Gould, PJ (2012). Open-Source Hardware Is a Low-Cost Alternative for Scientific Instrumentation and Research. *Modern Instrumentation*, 01(02), 8–20.

Gupta, J. B. (2009). *Theory & Performance Of Electrical Machines* (14th ed.). Delhi: SK Kataria & Sons.

Lockridge, G; Dzwonkowski, B; Nelson, R; Powers, S (2016). Development of a low-cost arduino-based sonde for coastal applications. *Sensors (Switzerland)*, 16(4), 1–16.

Mandal, S; Singh, D (2017). Real Time Data Acquisition of Solar Panel Using Arduino and Further Recording Voltage of the Solar Panel. *IJICS*, 7(3), 15–25.

Ofei, AK. (2010). Distribution Automation (DA) Using Supervisory Control and Data Acquisition (SCADA) with Advanced Metering Infrastructure (AMI). *Innovation Technology for Efficient and Reliable Electricity Supply*, 454–458. Waltham, MA: IEEE.

Park, J; John Park, ASD; Mackay, S (2003). *Practical data acquisition for instrumentation and control systems*. Newnes.

Sarma, P; Singh, HK; Bezboruah, T (2018). A Real-Time Data Acquisition System for Monitoring Sensor Data. *IJCSE*, 6(6), 539–542.

Siddique, A; Yadava, GS; Singh, B (2005). A review of stator fault monitoring techniques of induction motors. *IEEE Transactions on Energy Conversion*, Vol. 20, pp. 106–114.

Subha, M (2018). Artificial Intelligence Based Stator Winding Fault Estimation in Three Phase Induction Motor. *2018 Second ICECA Technology*, 1929–1933.